

Evidence of internal photoemission in the CO₂-laser-induced negative potential in homojunctions

M. López Sáenz

*Forschungsgesellschaft für Angewandte Naturwissenschaften e.V., Forschungsinstitut für Optik, Schloss Kressbach,
D-72072 Tübingen, Germany*

J. M. Guerra Pérez

Departamento de Optica, Facultad de Ciencias Fisicas, Universidad Complutense, Ciudad Universitaria, E-28040 Madrid, Spain

(Received 23 March 1995; revised manuscript received 12 June 1995)

A component of the strongly bias-dependent potential in the far-infrared laser-induced photoeffect produced in silicon and germanium homojunctions is reported. A model of laser-heated hot-carrier internal photoemission is presented. The model predictions are compared to experimental results, showing good agreement.

I. INTRODUCTION

The appearance of induced potentials in junctions irradiated by pulsed CO₂ lasers ($\lambda \approx 10.6 \mu\text{m}$) is well known.^{1,2} In recent work it has been observed that the photoresponse to the CO₂ light pulses is usually negative at the beginning, and then positive at the end of the induced signal.^{3,4} Here a negative photoresponse is a photoresponse that is opposite in sign to the normal photo-voltaic signal.

Umeno *et al.*¹ reported only the negative effect, and interpreted it as a laser-induced hot-electron effect. Conversely, Hasselbeck, Malone, and Kwok² observed only the positive effect, and interpreted it as a thermal effect in the junction resistance. Since then the positive effect has been studied and theoretically modeled as an impact-ionization laser-induced hot-electron effect.⁵

The negative effect has also been studied and modeled using energy balance equations modified by the laser heating of electrons.^{6,7} In the model proposed by Ashmontas and Shirmulis,^{6,7} the photoinduced potential is essentially bias independent. But the potential generated by the proposed mechanism must pass across the junction capacitance, which is, as is well known, strongly dependent on the bias potential. Thus a certain bias dependence in the measured effect is expected even if the induced potential is bias independent. In fact, a strong dependence of the negative effect on bias has been observed.^{1,6,7} The measurement and interpretation of the bias dependence of the negative effect is the object of our present study.

If the photoinduced potential is indeed bias independent, then upon passing across the junction capacitance it would change in the same manner as an equivalent externally generated electrical pulse. To test this hypothesis, electrical pulses synthesized with the same form as the laser light were applied to the junction to obtain the electrical response as a function of the bias. The bias dependence of the negative photoeffect was also measured. With a negative or small positive bias, synthesized electrical pulses and laser pulses exhibit the same behavior. However, with larger positive bias the photoeffect signal

is clearly stronger than the electrically stimulated response. A mechanism of internal photoemission by laser-heated hot carriers is proposed to explain the described behavior.

II. EXPERIMENTAL SETUP

A voltage pulse synthesizer is used to mimic the laser pulse shape. Single pulse mode measurements were performed to avoid progressive heating of the junction. The dc bias across the junction is isolated through capacitive coupling from the pulse synthesizer. The input electrical pulse and output were simultaneously recorded in a two-channel fast digitizer (2-G sample/s). All the circuit elements were connected with 50- Ω impedance coaxial cables.

A single transverse mode (TEM₀₀) CO₂ laser is used to excite the photoeffect in the junction. An electro-optic pulse slicer was used to obtain a 30-ns-wide optical pulse from the normally several- μs -wide laser pulse.

The measurements were taken in a single pulse mode, either directly with the transverse Gaussian profile of the TEM₀₀ mode, or by using a beam integrator in order to obtain a more homogeneous transverse profile.

As in previously reported measurements,⁸ the junction of a Slomons BPW 21 photodiode was used to induce the negative photoeffect. The BPW 21 is a silicon photodiode with a P⁺/N structure and a P⁺ doping of about $2 \times 10^{18} \text{ cm}^{-3}$. The junction is placed inside a Dewar cryostat at either room or liquid-N₂ temperature.

To obtain a sample of the excitation pulse, a ZnSe beam splitter and a 80-K-operated fast (5-ns rise time) Hg_xCd_{1-x}Te photodetector are used. The excitation pulse and photoresponse were recorded in the fast two-channel digitizer (Fig. 1).

III. EXPERIMENTAL RESULTS

Because the interesting behavior appears only for forward bias, here we will describe only the forward bias results. The 80- and 300-K electrical responses to the synthesized square potential pulses (with 30-ns pulse width)

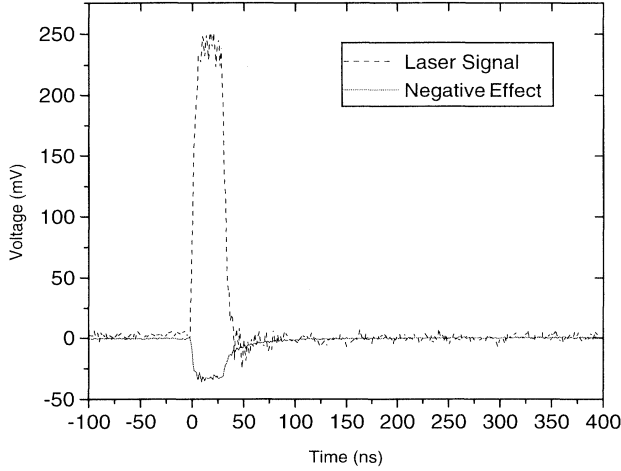


FIG. 1. Sliced laser light and induced photovoltage pulse shapes (the forward bias is 1 V).

are shown in Fig. 2, along with the corresponding negative photoresponses. The photoinduced signals measured at 80 K for two different radiation intensities can be seen in Fig. 3.

From an inspection of Fig. 2, we can see that electrical and optical responses are the same for reverse and small forward biases. For large forward bias, however, the photoresponse is much stronger than the electrical response, revealing the existence of an additional mechanism strongly dependent on the applied bias. These graphs show a sharp maximum somewhat below the transition potential of the junction at the corresponding lattice temperature. This mechanism is only noticeable at high forward bias. Because the effect is negative, the photoresponse should be related to the transport of the majority carriers across the junction.

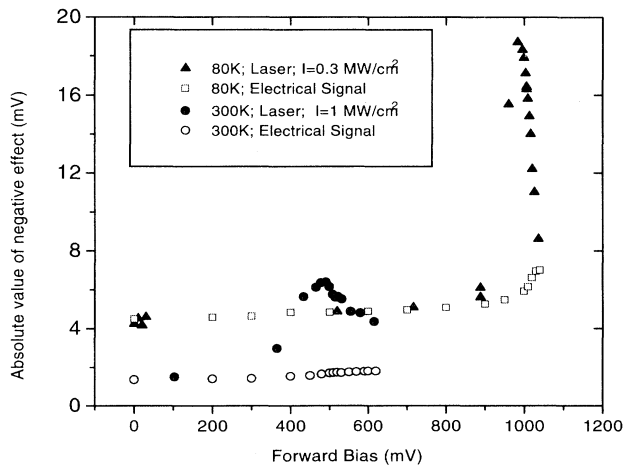


FIG. 2. Electrical responses: (▲) $T_L = 80$ K; (●) $T_L = 300$ K. Absolute value of the negative effect. The measurements with the beam integrator: (□) $T_L = 80$ K, $I = 0.3$ Mw cm⁻²; (○) $T_L = 300$ K, $I = 1$ Mw cm⁻².

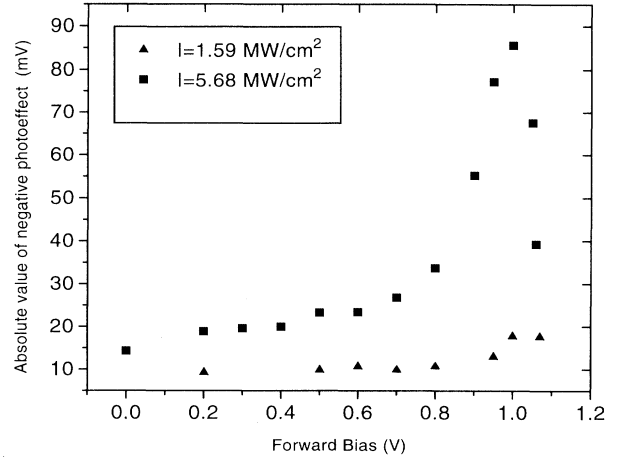


FIG. 3. Negative effect at two irradiation intensities as a function of bias voltage. The intensity is measured as the peak of the transverse Gaussian profile. The temperature was $T_L = 80$ K.

IV. INTERNAL PHOTOEMISSION EFFECT

To explain the above-described experimental results we propose a laser-heated hot-carrier internal photoemission model. As is well known, the primary effect of the infrared laser is to produce a heated plasma of carriers at a local thermal equilibrium temperature T_c , which can be much higher than the lattice temperature T_L .⁵ As a consequence of this carrier heating, a bias-independent effect appears that is described by Ashmontas and Shirmulis,^{6,7} and simulated with the electrical response in our experiment. The carrier heating, however, also excites some of the carrier population into levels near the top of the junction barrier, which can then be directly photoexcited to levels above the barrier.

The density of conduction electrons on the fringe, with high enough energies that could be photoexcited above the barrier, is (Fig. 4)

$$\Delta n = \int_{E_a}^{E_b} f_{FD} g_c(E) dE, \quad (1)$$

where

$$f_{FD} = \frac{1}{\exp\left(\frac{E - E_F}{KT_c}\right) + 1} \approx e^{-(E - E_F)/KT_c}, \quad (2)$$

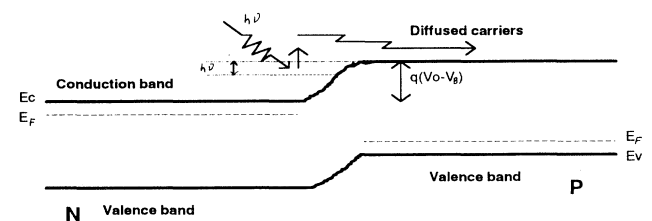


FIG. 4. Internal photoemission scheme.

$$g(E) = 4\pi \left[\frac{2m_e^*}{h^2} \right]^{3/2} (E - E_c)^{1/2}, \quad (3)$$

$$E_b = E_c + q(V_0 - V_B), \quad (4)$$

$$E_a = \begin{cases} E_c + q(V_0 - V_B) - h\nu & \text{if } q(V_0 - V_B) \geq h\nu \\ E_c & \text{if } q(V_0 - V_B) < h\nu. \end{cases} \quad (5)$$

Here m_e^* represents the electronic effective mass, E_F and E_c are the pseudo-Fermi-level of the hot-carrier plasma and the conduction-band energy, respectively, q is the electronic charge, and V_B and V_0 are the bias and transition voltages, respectively.

Using the scaled variable

$$x = \frac{E - E_c}{KT_c}, \quad (6)$$

we obtain

$$\Delta n = n \frac{2}{\sqrt{\pi}} \int_{a(V_B)}^{b(V_B)} x^{1/2} e^{-x} dx, \quad (7)$$

where

$$b(V_B) = \frac{q(V_0 - V_B)}{KT_c}, \quad (8)$$

$$a(V_B) = \begin{cases} \frac{q(V_0 - V_B) - h\nu}{KT_c} & \text{if } q(V_0 - V_B) \geq h\nu \\ 0 & \text{if } q(V_0 - V_B) < h\nu, \end{cases} \quad (9)$$

and

$$n = 2 \left[\frac{2\pi m_e^* KT_c}{h^2} \right]^{3/2} \exp \left[-\frac{E_c - E_F}{KT_c} \right]. \quad (10)$$

As

$$\int_0^\infty x^{1/2} e^{-x} dx = \frac{\sqrt{\pi}}{2},$$

the coefficient n can be identified as the density of carriers in the band. Equation (7), as illustrated in Fig. 5, has a sharp peak at a bias of

$$(V_B)_p = V_0 - \frac{h\nu}{q}. \quad (11)$$

The peak value is given by

$$(\Delta n)_p = \frac{2}{\sqrt{\pi}} n \int_0^{h\nu/KT_c} x^{1/2} e^{-x} dx = \frac{2}{\sqrt{\pi}} n \gamma \left(\frac{3}{2}, \frac{h\nu}{KT_c} \right), \quad (12)$$

where $\gamma(\alpha, x)$ is the incomplete gamma function. Equation (7) drops to zero when

$$(V_B)_0 = V_0. \quad (13)$$

Equation (12) shows explicitly the dependence of the peak value $(\Delta n)_p$ on T_c ; note that at low-carrier temperatures the effect should be more pronounced.

These characteristics are easily observed in the experimental results shown in Figs. 2 and 3. The carriers excit-

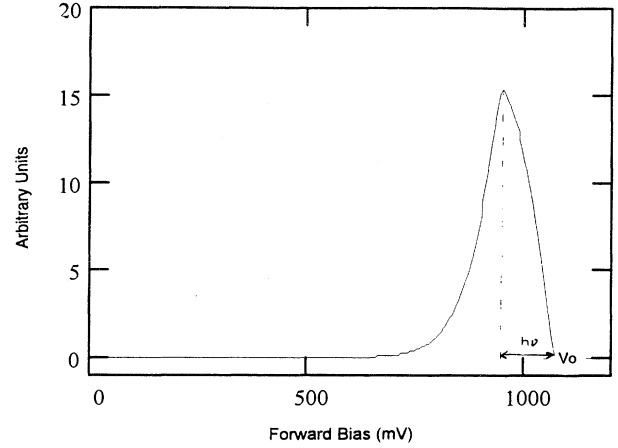


FIG. 5. Bias dependence of Eq. (7) for internal photoemission. $T_c = 500$ K, $V_0 = 1.075$ V, and $h\nu = 0.118$ eV.

ed in this range of energies may diffuse across the barrier, producing the observed effect. Thus the direct excitation of some carriers by the infrared laser light produces internal photoemission. When this occurs, the induced photocurrent is proportional to Δn as given by Eqs. (7)–(10). An equivalent expression can also be derived for holes.

Ignoring the influence of carrier transport (mobility, diffusivity, etc.) and optical (reflectivity, absorption cross section, etc.) properties in the generated photovoltage, the electrons and holes play a completely symmetric role. Thus the carriers making the highest contribution to the photoinduced negative potential in a P^+/N structure will be the holes. However, contributions from both carrier types in a P/N structure will be considered.

V. DISCUSSION AND CONCLUSIONS

In order to isolate the internal photoemission effect we have subtracted the electrical response from the photoin-

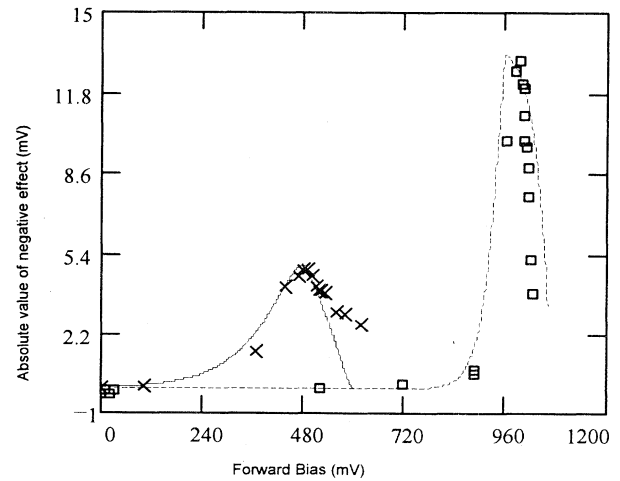


FIG. 6. Fit to the internal photoemission effect shown in Fig. 2 (the measurements with the beam integrator) by Eq. (7). (\times) $T_L = 300$ K, $I = 1$ MW cm^{-2} ; the fit parameters are $T_c = 900$ K, $V_0 = 0.6$ V. (\square) $T_L = 80$ K, $I = 0.3$ MW cm^{-2} ; the fit parameters are $T_c = 290$ K, $V_0 = 1.07$ V.

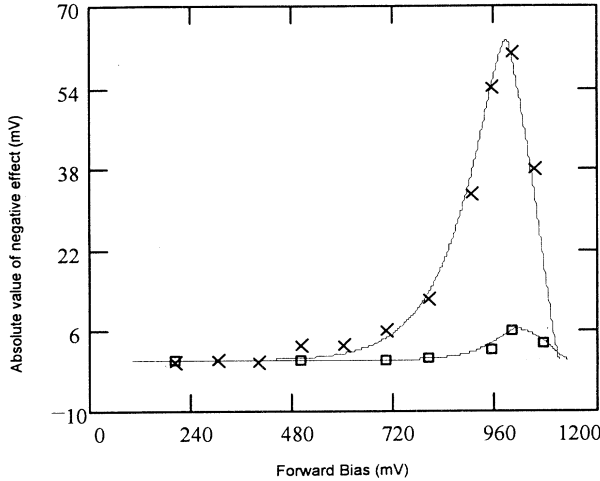


FIG. 7. Fit to the internal photoemission effect shown in Fig. 3 (the intensity is measured as the peak of the transverse Gaussian profile) by Eq. (7). (×) $T_L = 80$ K, $I = 5.68$ MW cm⁻²; the fit parameters are $T_c = 900$ K, $V_0 = 1.11$ V. (□) $T_L = 80$ K, $I = 1.59$ MW cm⁻²; the fit parameters are $T_c = 600$ K, $V_0 = 1.13$ V.

duced one. A fit is then made to Eq. (7), the internal photoemission. These fits are shown in Figs. 6, 7, and 8. As can be seen, the equation fits the data remarkably well, clearly supporting our theoretical interpretation. The magnitudes V_0 and T_c were used as the parameters in the fit. The equation is also very sensitive to the $h\nu$ value, and here we have used $h\nu = 0.118$ eV, which corresponds to a wavelength of 10.6 μ m.

The photoresponse measured at $T_L = 300$ K proved to be the most difficult data to fit. In particular, the fit for the photoresponse with the highest bias is not very good. The photoresponse at the falling edge of the peak has been apparently enhanced, but the detailed mechanism giving place to this behavior is not clear. The theoretical model predicts a reduction in the photoresponse as T_L is increased (Fig. 6). The increase in the carrier temperature corresponding to this fit is $\Delta T_c \approx 600$ K ($=900 - 300$). The optical integrator provides a very smooth intensity distribution across the irradiated area, and the average peak irradiation intensity used in the measurements at $T_L = 300$ K was estimated to be about 1 MW cm⁻². The fit corresponding to $T_L = 80$ K gives a carrier temperature increase $\Delta T_c \approx 210$ K, for a radiation intensity of 0.3 MW cm⁻².

Because the carrier thermal distribution is not degenerated, it can be expected that the carrier plasma retains a sizable fraction of the absorbed radiation energy. In a previous work⁵ we demonstrated that if the carrier plasma remained in equilibrium under excitation by radiation and acoustical-phonon losses, then

$$\frac{T_c}{T_L} = 1 + \frac{I}{I_0}, \quad (14)$$

and hence

$$\frac{I}{I'} = \frac{T_c - T_L}{T'_c - T_L} = \frac{\Delta T_c}{\Delta T'_c}. \quad (15)$$

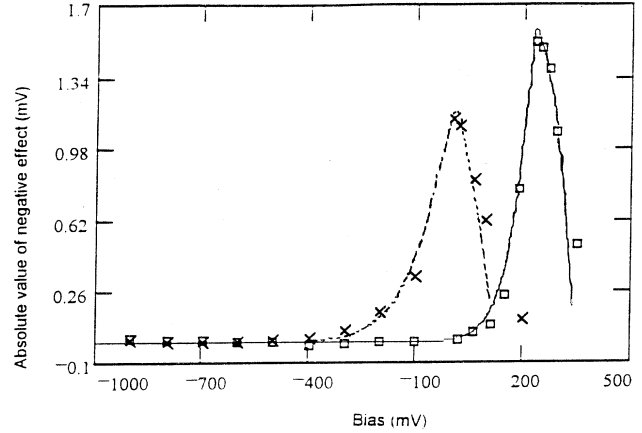


FIG. 8. Fit to the internal photoemission effect reported by Umeno *et al.* for a germanium junction (Ref. 1) by Eq. (7). (×) $T_L = 311$ K; the fit parameters are $T_c = 770$ K, $V_0 = 0.13$ V. (□) $T_L = 240$ K; the fit parameters are $T_c = 450$ K, $V_0 = 0.35$ V.

In the above case, this means

$$\frac{1 \text{ MW cm}^{-2}}{0.3 \text{ MW cm}^{-2}} \approx \frac{600}{210}.$$

The fit results support this carrier plasma equilibrium assumption. The fitted values ($V_0 \approx 0.6$ V) for the transition potential at room temperature and at 80 K ($V_0 \approx 1.075$ V) are also reasonable.

In Fig. 8 a fit was made to some experimental results reported by Umeno *et al.*,¹ measured in germanium junctions. The fit at $T_L = 300$ K shows the same problem observed in the silicon junctions with large forward bias at the same temperature. Important practical consequences are evident from our model results. Perhaps the most striking result is that any forward-biased junction at the $[V_0 - (h\nu/q)]$ potential could be a good photosensor for far-infrared radiation. From Eq. (7), the higher the N⁺ or P⁺ doping is, the higher the foreseeable effect.

In conclusion, here we have provided much evidence supporting the existence, at high forward bias, of an important internal photoemission contribution to the negative photoinduced effect in silicon and germanium junctions produced by far-infrared laser light.

ACKNOWLEDGMENTS

We are very grateful to Dr. F. Encinas for interesting discussions relating to the subject of this paper. This work was partially supported by the "C.I.C.Y.T." under the Project No. MAT93-0150 grant to the University Complutense of Madrid. The experimental part of this research was conducted at the FGAN-Forschungsinstitut für Optik in Tübingen, Germany. We would like to express our appreciation to the institute for allowing us to use their facilities and expertise. In particular we would like to thank Dr. D. H. Höhn, the director, and Dr. R. Ebert for his help in the laboratory and for his many useful suggestions, as well as Ing. R. Frank for his advice and help with the electronics.

- ¹M. Umeno, Y. Sugito, T. Jimbo, H. Hattori, and Y. Amemiya, *Solid State Electron.* **21**, 191 (1978).
- ²M. Hasselbeck, D. P. Malone, and H. S. Kwok, *Appl. Opt.* **21**, 2769 (1983).
- ³E. Dominguez Ferrari, F. Encinas Sanz, and J. M. Guerra Perez, *IEEE Photogr. Tech. Lett.* **1**, 469 (1989).
- ⁴E. Dominguez Ferrari, F. Encinas Sanz, and J. M. Guerra Perez, *Phys. Rev. B* **42**, 11 714 (1990).
- ⁵F. Encinas Sanz, J. M. Guerra Perez, and E. Dominguez Ferrari, *Phys. Rev. B* **47**, 4517 (1993).
- ⁶S. P. Ashmontas and E. I. Shirmulis, *Izv. Akad. Nauk. SSSR Ser. Fiz.* **49**, 1162 (1985) [*Bull. Acad. Sci. USSR Phys. Ser.* **49**, 115 (1985)].
- ⁷S. P. Ashmontas and E. I. Shirmulis, *Fiz. Tekh. Poluprovodn.* **20**, 2212 (1985) [*Sov. Phys. Semicond.* **20**, 1382 (1986)].
- ⁸F. Encinas Sanz, J. M. Guerra Perez, and E. Dominguez Ferrari, *IEEE J. Quantum Electron.* **29**, 1223 (1993).